

Status report of the baseline collimation system of CLIC. Part I

J. Resta-López¹, D. Angal-Kalinin², B. Dalena³,
J. L. Fernández-Hernando², F. Jackson², D. Schulte³, A. Seryi¹
and R. Tomás³

¹JAI, University of Oxford, UK

²STFC, Daresbury, UK

³CERN, Geneva, Switzerland

E-mail: j.restalopez@physics.ox.ac.uk

Abstract. Important efforts have recently been dedicated to the characterisation and improvement of the design of the post-linac collimation system of the Compact Linear Collider (CLIC). This system consists of two sections: one dedicated to the collimation of off-energy particles and another one for betatron collimation. The energy collimation system is further conceived as protection system against damage by errant beams. In this respect, special attention is paid to the optimisation of the energy collimator design. The material and the physical parameters of the energy collimators are selected to withstand the impact of an entire bunch train. Concerning the betatron collimation section, different aspects of the design have been optimised: the transverse collimation depths have been recalculated in order to reduce the collimator wakefield effects while maintaining a good efficiency in cleaning the undesired beam halo; the geometric design of the spoilers has been reviewed to minimise wakefields; in addition, the optics design has been optimised to improve the collimation efficiency. This report presents the current status of the the post-linac collimation system of CLIC. Part I of this report is dedicated to the study of the CLIC energy collimation system.

1. Introduction

The post-linac collimation systems of the future linear colliders will play an essential role in reducing the detector background at the interaction point (IP), and protecting the machine by minimising the activation and damage of sensitive accelerator components.

The CLIC Beam Delivery System (BDS), downstream of the main linac, consists of a 370 m long diagnostics section, an almost 2000 m long collimation system, and a 460 m long Final Focus System (FFS) [1, 2]. Figure 1 shows the betatron and dispersion functions along the CLIC BDS. Some relevant CLIC design parameters are shown in Table 1 for the options at 500 GeV and 3 TeV centre-of-mass (CM) energy.

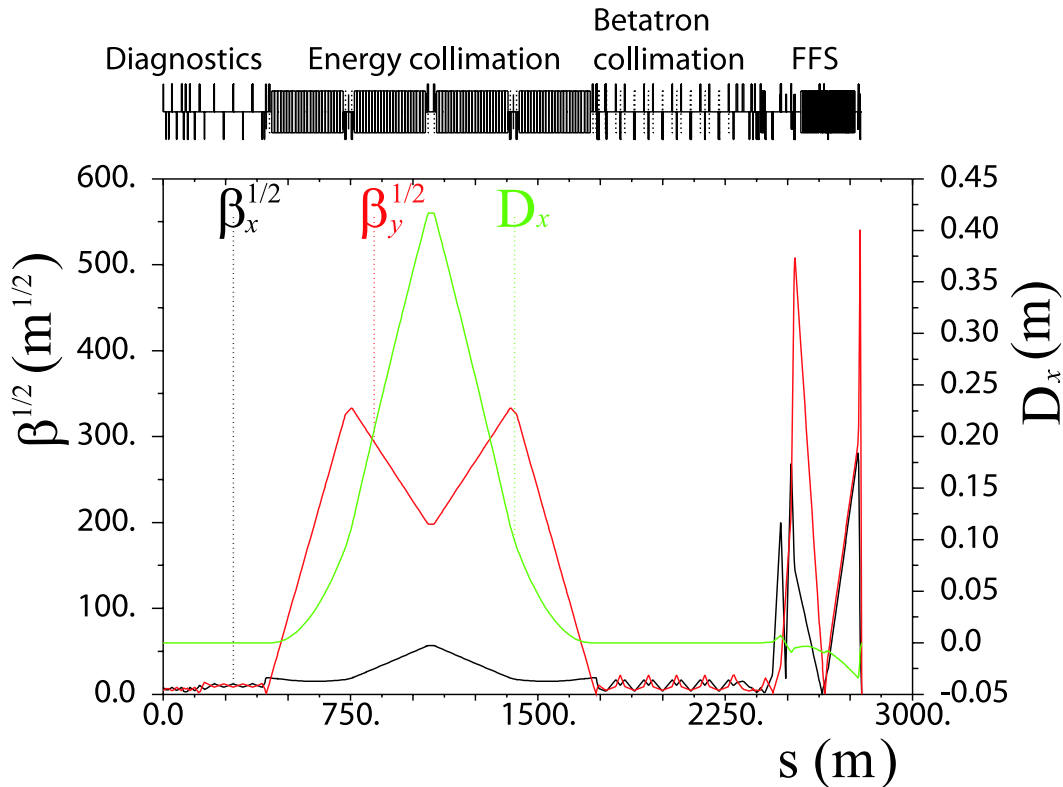


Figure 1. Optical functions of the CLIC beam delivery system.

In the CLIC BDS there are two collimation sections:

- The first post-linac collimation section is dedicated to energy collimation. The energy collimation depth is determined by failure modes in the linac [3]. A spoiler-absorber scheme (Fig. 2), located in a region with non-zero horizontal dispersion, is used for intercepting miss-steered or errant beams with energy deviation larger than 1.3% of the nominal beam energy.
- Downstream of the energy collimation section, a dispersion-free section, containing eight spoilers and eight absorbers, is dedicated to the cleaning of the transverse halo of the beam, thereby reducing the experimental background at the IP.

Table 1. CLIC parameters at 0.5 TeV and 3 TeV CM energy.

Parameter	CLIC 0.5 TeV	CLIC 3 TeV
Design luminosity ($10^{34} \text{ cm}^{-2}\text{s}^{-1}$)	2.3	5.9
Linac repetition rate (Hz)	50	50
Particles/bunch at IP ($\times 10^9$)	6.8	3.72
Bunches/pulse	354	312
Bunch length (μm)	72	44
Bunch separation (ns)	0.5	0.5
Bunch train length (ns)	177	156
Emittances $\gamma\epsilon_x/\gamma\epsilon_y$ (nm rad)	2400/25	660/20
Transverse beam sizes at IP σ_x^*/σ_y^* (nm)	202/2.3	45/0.9
BDS length (km)	1.73	2.79

The spoilers are thin devices ($\lesssim 1$ radiation length) which scrape the beam halo and, if accidentally struck by the full power beam, will increase the volume of the phase space occupied by the incident beam via multiple Coulomb scattering. In this way, the transverse density of the scattered beam is reduced for passive protection of the downstream absorber. The absorbers are usually thick blocks of material (of about 20 radiation length) designed to provide efficient halo absorption or complete removal of potentially dangerous beams.

The optics of the CLIC collimation system was originally designed by rescaling of the optics of the collimation system of the previous Next Linear Collider (NLC) project at 1 TeV centre-of-mass energy [4, 5] to the 3 TeV CLIC requirements. In the present CLIC baseline optics the length of the energy collimation section has been scaled by a factor 5 and the bending angles by a factor 1/12 with respect to the 1 TeV NLC design [6]. On the other hand, the optics of the CLIC betatron collimation section was not modified with respect to the original design of the NLC.

It is worth mentioning that, unlike the International Linear collider (ILC) [7], where the betatron collimation section is followed by the energy collimators, in CLIC the energy collimation section is upstream of the betatron one. The main reason of choosing this lattice structure is because miss-phased or unstable off-energy drive beams are likely failure modes in CLIC, and they are expected to be much more frequent than large betatron oscillations with small emittance beams. Therefore, the energy collimation system is conceived as the first post-linac line of defence for passive protection against off-energy beams in the CLIC BDS.

Recently many aspects of the CLIC collimation system design have been reviewed and optimised towards a consistent and robust system for the Conceptual Design Report of CLIC (CLIC CDR), to be completed during 2011. In this report we describe the current status of the CLIC collimation system at 3 TeV CM energy. Here we mainly focus on the description of the collimation layout and the optimisation of the necessary

parameters of the baseline design to improve the collimation performance, only taking into account the primary beam halo. The aim is to define basic specifications of the design. Studies including secondary particle production and muon collimation are described elsewhere [8, 9]. Part I of this report is dedicated to the study of the CLIC energy collimation system.

2. Energy collimation

The beam power of the CLIC beam in the BDS with nominal parameters at 3 TeV CM energy is about 14 MW. The sustained disposal of such a high beam power during beam operation is a challenging task. Operation failures might generate errant beams which can hit and damage machine components. Therefore, machine protection, based on active and passive strategies, is required. The general CLIC Machine protection strategies are described in [10].

The CLIC energy collimation section is conceived to fulfil a function of passive protection in the BDS against miss-steered or errant beams coming from the main linac. The energy collimation depth is determined by fast failure modes which result in a significant energy deviation of the beam. For instance, possible CLIC fast (‘in flight’) failure modes scenarios can be caused by the effect of a missing drive beam, injection phase errors and changes in the charge of the main beam [3].

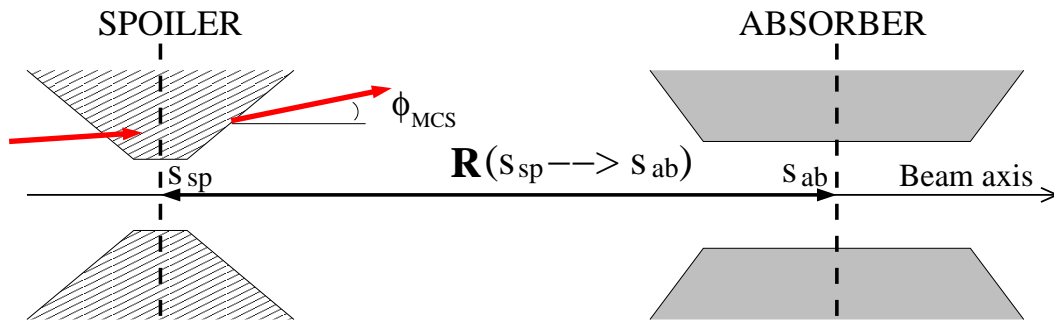


Figure 2. Basic spoiler-absorber scheme.

The CLIC energy collimation system consists of a spoiler-absorber scheme (see Fig. 2), located in a region with non-zero horizontal dispersion. The lattice layout of the CLIC energy collimation section is shown in Fig. 3. The corresponding optical parameters and transverse beam size at the energy spoiler and absorber are indicated in Table 2.

The selection of the material to make the spoiler is basically determined by the electrical, thermal and mechanical properties of the material. Regarding the survival condition of the energy spoiler, the robustness of the material is crucial. At the same time, a spoiler with high electrical conductivity is desired to avoid intolerable wakefield effects. Earlier studies of the CLIC spoiler heating and spoiler damage limit [11] concluded that a spoiler made of beryllium (Be) might be a suitable solution in terms

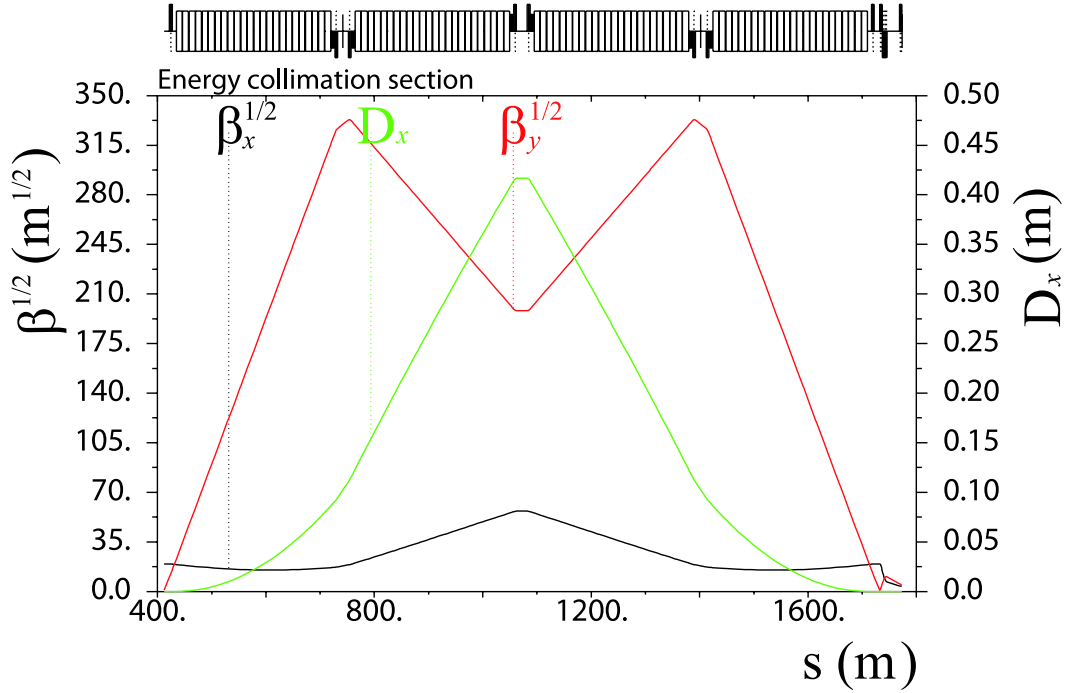


Figure 3. Optical functions of the CLIC energy collimation section: horizontal dispersion and square root of the betatron functions.

Table 2. Optics and beam parameters at collimator position for energy collimation: longitudinal position (s), horizontal and vertical β -functions (β_x and β_y), horizontal dispersion (D_x), horizontal and vertical rms beam sizes (σ_x and σ_y). In this case a uniform energy distribution with 1% full width energy spread has been considered.

Name	s [m]	β_x [m]	β_y [m]	D_x [m]	σ_x [μm]	σ_y [μm]
ENGYSP (spoiler)	907.098	1406.33	70681.87	0.27	779.626	21.945
ENGYAB (absorber)	1072.098	3213.03	39271.54	0.416	1201.189	16.358

of high robustness and acceptable wakefields. On the other hand, in the current design the CLIC absorbers are made of titanium alloy (90% Ti, 6% Al, 4% V) with copper (Cu) coating.

The collimation depth of the spoiler has been set to intercept beams with energy deviation larger than 1.3% of the nominal beam energy. The horizontal aperture for the energy collimator is then set to $a_x = D_x \delta_{\text{aper}}$, with D_x the horizontal dispersion at the spoiler position and $\delta_{\text{aper}} = \pm 1.3\%$.

It is necessary to point out that the energy collimation system, with a total length of 1400 m, is the longest part of the BDS. This space is filled almost entirely with bending magnets to generate the required horizontal dispersion. The length of the energy collimation system is determined by a trade-off between the following requirements:

- The beam spot size at the collimators must be sufficiently large for passive

protection. The energy collimators are required to withstand the impact of a full bunch train of nominal emittance.

- The emittance growth due to synchrotron radiation emission must be constrained within tolerable levels.
- the half gap a_x must be big enough to minimise the near-axis wakefield effects on the beam during normal operation of the machine.

For a given lattice the horizontal emittance growth due to incoherent synchrotron radiation can be evaluated using the following expression [12]:

$$\Delta(\gamma\epsilon_x) \simeq (4.13 \times 10^{-8} \text{ m}^2\text{GeV}^{-6})E^6 I_5, \quad (1)$$

as a function of the beam energy E and the so-called radiation integral I_5 , which is defined as [13],

$$I_5 = \int_0^L \frac{\mathcal{H}}{|\rho_x^3|} ds = \sum_i L_i \frac{\langle \mathcal{H} \rangle_i}{|\rho_{x,i}^3|}, \quad (2)$$

where the sum runs over all bending magnets, with bending radius ρ_i , length L_i , and the average of the function \mathcal{H} , which is defined by:

$$\mathcal{H} = \frac{D_x^2 + (D'_x\beta_x + D_x\alpha_x)^2}{\beta_x}, \quad (3)$$

where β_x and $\alpha_x = -(1/2)d\beta_x/ds$ denote the typical twiss parameters, D_x the dispersion function and $D'_x = dD_x/ds$.

For the CLIC collimation system $I_5 \simeq 1.9 \times 10^{-19} \text{ m}^{-1}$, and then $\Delta(\gamma\epsilon_x) \simeq 0.089 \text{ } \mu\text{m}$. This means about 13.5% emittance growth respect to the design emittance $\gamma\epsilon_x = 0.66 \text{ } \mu\text{m}$. This corresponds to a beam core luminosity loss of $\Delta\mathcal{L}/\mathcal{L}_0 = 1 - 1/\sqrt{1 + \Delta(\gamma\epsilon_x)/(\gamma\epsilon_x)} \simeq 6\%$. For the total CLIC BDS (including the CLIC collimation system and the FFS) it results $I_5 \simeq 3.8 \times 10^{-19} \text{ m}^{-1}$ and an emittance growth of $\Delta(\gamma\epsilon_x)/(\gamma\epsilon_x) \simeq 27.3\%$. This translates into a total luminosity loss of about 11.4%. This value is much lower than the result of 24% obtained in Ref. [14] from beam tracking simulations. This discrepancy is basically due to the fact that our calculation from Eqs. (1) only considers the effect from the radiation emission due to the deflection of the beam by the bending magnets, while the tracking simulations also take into account the additional effect from the optical nonlinearities of the lattice.

In the following sections we describe the design of the spoiler and absorber based on survival considerations and, by means of simulations, the thermo-mechanical performance of the spoiler is investigated in detail for the worst damage scenario from a full bunch train impact. Collimation efficiency simulation studies are also performed in order to optimise the collimation apertures.

2.1. Spoiler and absorber design

This section is devoted to the optimisation of the geometric dimensions of the energy spoiler and absorber, considering the geometry of Fig. 4. The design parameters of the energy spoiler and absorber are shown in Table 3.

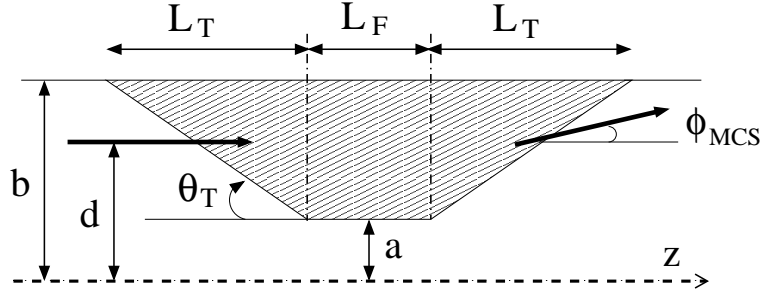


Figure 4. Spoiler and absorber jaw longitudinal view.

Table 3. Design parameters of the CLIC energy spoiler and absorber.

Parameter	ENGYSP (spoiler)	ENGYAB (absorber)
Geometry	Rectangular	Rectangular
Hor. half-gap a_x [mm]	3.51	5.41
Vert. half-gap a_y [mm]	8.0	8.0
Tapered part radius b [mm]	8.0	8.0
Tapered part length L_T [mm]	90.0	27.0
Taper angle θ_T [mrad]	50.0	100.0
Flat part length L_F [radiation length]	0.05	18.0
Material	Be	Ti alloy–Cu coating

2.1.1. *Absorber protection.* The main function of the spoiler is to provide sufficient beam angular divergence by multiple Coulomb scattering (MCS) to decrease the transverse density of an incident beam, thereby reducing the damage probability of the downstream absorber and any other downstream component. This condition determines the minimum length of the material traversed by the beam in the spoiler, i.e. the flat part of the spoiler body ($L_F \neq 0$).

Beam particles traversing the spoiler material are deflected by MCS. The transverse root mean square (rms) scattering angle experienced by the beam particle at the exit of the spoiler can be calculated using the well known Gaussian approximation of the Molière formula [15]:

$$\phi_{MCS} = \frac{13.6 \text{ [MeV]}}{\beta c p} z \sqrt{\frac{\ell}{X_0}} \left[1 + 0.038 \ln \left(\frac{\ell}{X_0} \right) \right], \quad (4)$$

where X_0 is the radiation length of the spoiler material, ℓ is the length of material traversed by the beam particle, β is the relativistic factor ($\beta \simeq 1$ for ultra-relativistic beams), c the speed of light, p the beam momentum, and z is the charge of the incident particle ($z = 1$ for electrons and positrons). Equation (4) is accurate to 11% or better for $10^{-3} < \ell/X_0 < 100$. The square of the transverse angular divergence of a beam at the exit of the spoiler is given by $\langle x_{sp}^{\prime 2} \rangle = \langle x_{sp0}^{\prime 2} \rangle + \phi_{MCS}^2$, and $\langle y_{sp}^{\prime 2} \rangle = \langle y_{sp0}^{\prime 2} \rangle + \phi_{MCS}^2$ for the

horizontal and vertical plane, respectively. The terms $\langle x_{sp0}^2 \rangle$ and $\langle y_{sp0}^2 \rangle$ refer to the initial angular components at the entrance of the spoiler and are usually much smaller than the scattering angular component. Taking into account the linear transport, the expected value of the square of the horizontal and vertical displacements at the downstream absorber can be approximated by

$$\langle x_{ab}^2 \rangle \simeq R_{12}^2(s_{sp} \rightarrow s_{ab})\phi_{MCS}^2 + D_x^2\sigma_\delta^2, \quad (5)$$

$$\langle y_{ab}^2 \rangle \simeq R_{34}^2(s_{sp} \rightarrow s_{ab})\phi_{MCS}^2. \quad (6)$$

In Eq. (5) the dispersive component $D_x^2\sigma_\delta^2$ has been taken into account, with $D_x = 0.416$ m the horizontal dispersion at the energy absorber position, and $\sigma_\delta = \sqrt{\langle \delta_E^2 \rangle - \langle \delta_E \rangle^2}$ the rms beam energy spread. $\delta_E \equiv \Delta E/E_0$ represents the energy deviation, with E_0 the nominal beam energy. $R_{12}(s_{sp} \rightarrow s_{ab}) = 160.75$ m and $R_{34}(s_{sp} \rightarrow s_{ab}) = 169.26$ m are the corresponding linear transfer matrix elements between the energy spoiler and absorber. For beam energy 1500 GeV and length of the spoiler material $\ell < 1 X_0$ the rms angular divergence by MCS is $\phi_{MCS} \sim 1 \mu\text{rad}$. If one considers energy spread values $\sigma_\delta \approx 0.29\%$, the energy dispersive term $D_x\sigma_\delta$ is dominant in Eq. (5), and we can approximate the transverse beam size at the absorber position s_{ab} by:

$$\sigma_x(s_{ab}) = \sqrt{\langle x_{ab}^2 \rangle} \simeq D_x\sigma_\delta, \quad (7)$$

$$\sigma_y(s_{ab}) = \sqrt{\langle y_{ab}^2 \rangle} \simeq R_{34}(s_{sp} \rightarrow s_{ab})\phi_{MCS}. \quad (8)$$

For the protection of an absorber made of Ti alloy, the following limit for the radial beam size can be established [4, 16]:

$$\sigma_r(s_{ab}) = \sqrt{\sigma_x(s_{ab})\sigma_y(s_{ab})} \gtrsim 600 \mu\text{m}. \quad (9)$$

Using Eqs. (7) and (8), the constraint (9) can be rewritten as follows:

$$\sqrt{|R_{34}(s_{sp} \rightarrow s_{ab})|D_x\sigma_\delta\phi_{MCS}} \gtrsim 600 \mu\text{m}. \quad (10)$$

In terms of the transverse particle density peak, the condition for absorber survival can be written as:

$$\hat{\rho}(s_{ab}) = \frac{N_e}{2\pi\sigma_r^2(s_{ab})} \lesssim 1.64 \times 10^9 \text{ particles/mm}^2 \text{ per bunch}, \quad (11)$$

where $N_e = 3.72 \times 10^9$ is the number of particles per bunch.

Considering a Gaussian beam energy distribution with $\sigma_\delta = 0.5\%$ energy spread width, from the constraint (10) one obtains that $\phi_{MCS} \gtrsim 10^{-6}$ rad ensures the absorber survival. From this condition and using Eq. (4) one can determine the minimum length of spoiler material necessary to guarantee the absorber survival. This condition is fulfilled if the Be spoiler (Fig. 4) is designed with a central flat part of length $L_F \gtrsim 0.02 X_0$.

Similar results are obtained considering a beam with a uniform energy distribution of $A_\delta = 1\%$ full energy spread and where $\sigma_\delta = A_\delta/\sqrt{12}$.

In order to validate these results tracking simulations of bunches have been performed through the CLIC BDS, with 50000 macroparticles per bunch, using the code PLACET [17]. In this beam model a macroparticle represents a large number of electrons (or positrons) with nearly the same energy and phase space position. For instance, macroparticle i is represented by a 6-D phase space vector $(x_i, x'_i, y_i, y'_i, z_i, E_i)$, by a number of second moments[‡], and by a weight proportional to the number of particles it represents.

Assuming all particles of the beam hit the energy spoiler and full beam transmission through the spoiler, and applying MCS, we have calculated the transverse beam spot size $\sigma_r = \sqrt{\sigma_x \sigma_y}$ and its corresponding transverse beam density at the energy absorber. From the tracking simulations of the 50000 macroparticles of one bunch, σ_x and σ_y are calculated from the rms of the x and y positions of the macroparticle distribution. Figure 5 compares the result of σ_r at the absorber position as a function of the spoiler length (in units of radiation length) traversed by the beam for the following cases: a monochromatic beam, i.e. with no energy spread, and a beam with a uniform energy distribution of 1% full spread. The results from the tracking simulations are compared with those from analytical calculations using Eqs. (7) and (8). The corresponding results in terms of transverse particle density are shown in Fig. 6. For a realistic case of a beam with 1% of energy spread, selecting a length for the energy spoiler of about $0.05 X_0$ might be enough to ensure the survivability of the downstream absorber in case of a full impact of the beam.

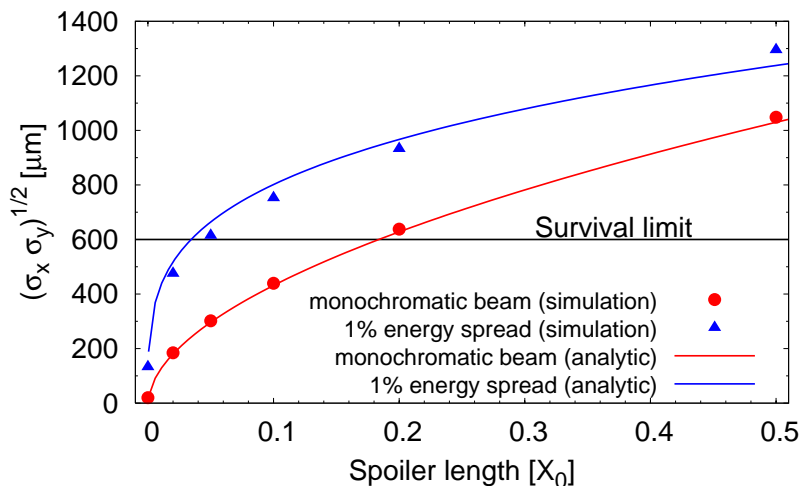


Figure 5. Transverse spot size at the energy absorber position as a function of the upstream spoiler length.

[‡] The second moments are the covariances of transverse phase coordinates for all particles represented by the macroparticle.

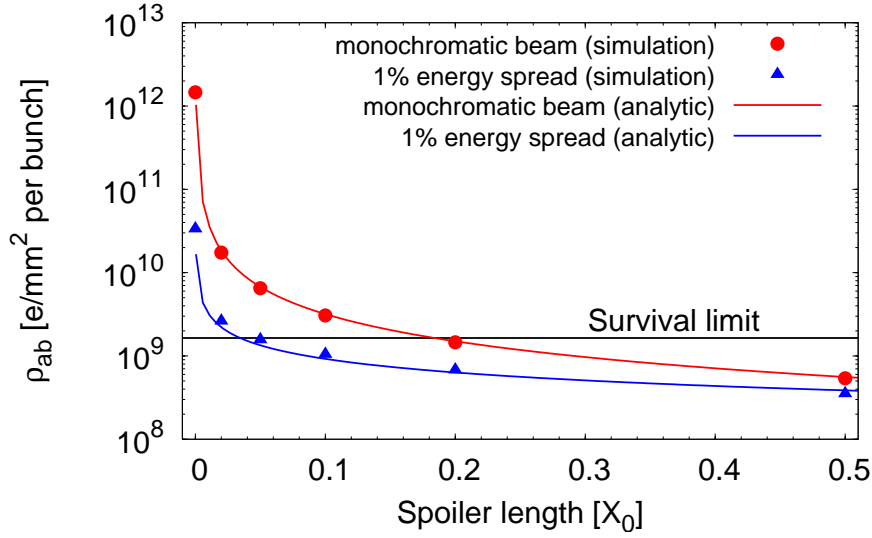


Figure 6. Transverse beam density at the energy absorber position as a function of the upstream spoiler length.

2.1.2. Spoiler protection. Based on the SLC experience[§], energy errors in the linac are expected to occur much more frequently than orbit disruptions of on-energy beams. Therefore, the E-spoiler has to be designed robust enough so that it survives without damage from the impact of an entire bunch train in case of likely events generating energy errors.

The instantaneous heat deposition is the principal mechanism leading to spoiler/collimator damage. The main sources of such a heating are the energy deposition by direct beam-spoiler material interaction, the image current heat deposition and the electric field breakdown. The most critical case is the instantaneous temperature rise in the spoiler due to a deep beam impact. Since the thickness of the spoiler is significantly small in terms of radiation length ($L_F \ll 1 X_0$), electrons/positrons deposit energy basically by ionization, and practically no electromagnetic showers are developed.

As an approximate criterion for spoiler survival the following condition can be established: the instantaneous temperature increment due to the impact of a full bunch train on the spoiler ($\Delta\hat{T}_{\text{inst}}$) must be lower than the temperature excursion limit for melting (ΔT_{melt}) and the temperature excursion limit for fracture of the material by thermal stress (ΔT_{fr}), i.e.

$$\Delta\hat{T}_{\text{inst}} = \frac{1}{\varrho C_p} \left(\frac{dE}{dz} \right) \frac{N_e N_b}{2\pi\sigma_x\sigma_y} < \min[\Delta T_{\text{fr}}, \Delta T_{\text{melt}}], \quad (12)$$

where ϱ is the density of the spoiler material, C_p is the heat capacity, N_e the bunch population and N_b the number of bunches per train. The safe limit is below the minimum between the thermal stress temperature limit ΔT_{fr} and the melting limit ΔT_{melt} . Generally the minimum corresponds to ΔT_{fr} .

[§] The Stanford Linear Collider (SLC) [18] is the sole linear collider built to date.

Here the energy deposition per unit length is denoted as (dE/dz) , whose value can be determined using the formula for the collision stopping power given in Ref. [19] in the high energy limit:

$$\frac{1}{\varrho} \left(\frac{dE}{dz} \right) = 0.153536 \frac{Z}{A} B(T) , \quad (13)$$

where Z/A is the ratio of the number of electrons in the atom to the atomic weight of the spoiler material, and $B(T)$ is the stopping number defined in [19]. It is necessary to mention that Eq. (13) gives a conservative estimation of the energy deposited in the spoiler and overestimates it, since by definition the stopping power is the energy lost by the passing beam, and not the energy that is actually deposited in the target. A fraction of the lost energy might indeed escape from the spoiler.

Table 4 shows the instantaneous increment of temperature calculated using Eqs. (12) and (13) for CLIC electron and positron beams and for different spoiler materials. For these calculations we have neglected the temperature dependence of the heat capacity C_p and used the following rms transverse beam sizes: $\sigma_x = 779.6 \mu\text{m}$ and $\sigma_y = 21.9 \mu\text{m}$. The material properties of Table 5 have been considered. These material data have been obtained from Ref. [20].

Table 4. Energy deposition per unit length (dE/dz) estimated from Eq. (13) for a CLIC beam traversing a thin spoiler, and instantaneous temperature increment calculated using Eq. (12). Different spoiler materials are compared.

Spoiler Material	Electron beam		Positron beam	
	dE/dz [MeV/cm]	$\Delta\hat{T}_{inst}$ [K]	dE/dz [MeV/cm]	$\Delta\hat{T}_{inst}$ [K]
Be	4.4003	214	4.3181	209
C	6.001	648	5.8879	636
Ti	10.8487	786	10.6406	770
Cu	20.9522	1049	20.5422	1028
W	39.1714	2606	38.3897	2554

Table 5. Material properties: atomic number Z , mass number A , material density ϱ , specific heat capacity C_p , electrical conductivity σ (at room temperature, 293 K) and radiation length X_0 .

Material	Z	A [g/mol]	ϱ [gm^{-3}]	C_p [$\text{Jg}^{-1}\text{K}^{-1}$]	σ [$\Omega^{-1}\text{m}^{-1}$]	X_0 [m]
Be	4	9.01218	1.84×10^6	1.925	2.3×10^7	0.353
C	6	12.0107	2.25×10^6	0.708	1.7×10^4	0.188
Ti	22	47.867	4.5×10^6	0.528	1.8×10^6	0.036
Cu	29	63.546	8.93×10^6	0.385	5.9×10^7	0.014
W	74	183.84	19.3×10^6	0.134	1.8×10^7	0.0035

The rapid heating of the material caused by the impact of the train in the spoiler may contribute to the fracture of the material by thermal stress. The increment of temperature which determines the limit for thermal fracture can be analytically evaluated using the following expression:

$$\Delta T_{\text{fr}} \cong \frac{2\sigma_{\text{UTS}}}{\alpha_T Y}, \quad (14)$$

where σ_{UTS} is the ultimate tensile strength, α_T is the thermal expansion coefficient and Y is the modulus of elasticity (or Young modulus). The ultimate tensile strength is defined as the maximum stress that the material can withstand. It is necessary to mention that for the value of σ_{UTS} discrepancies of up to 40% can be found between different bibliographic sources about material data. Here we have used the material information from Ref. [20], which gives a pesimistic value for σ_{UTS} in comparison with other bibliographic sources.

For the CLIC energy spoiler made of Be, using the mechanical and thermal properties of Table 6, we obtain $\Delta T_{\text{fr}} \simeq 228$ K, which is slightly bigger than the values obtained for $\Delta \hat{T}_{\text{inst}}$ for a Be spoiler (see Table 4). Therefore, according this analytic calculation the Be spoiler is below, but close, the fracture limit in case of the impact of an entire CLIC bunch train.

Table 6. Summary of material properties for beryllium.

Young modulus, Y [10^5 MPa]	2.87
Thermal expansion coefficient, α_T [10^{-6} K $^{-1}$]	11.3
Ultimate tensile strength, σ_{UTS} [MPa]	370
Tensile yield strength [MPa]	240
Compressive yield strength [MPa]	270
Specific heat capacity, C_p [J/(gK)]	1.925
Density, ρ [g/cm 3]	1.84

In general Eq. (14) may be a good approximation to estimate the temperature at which the material may crack. However, it is necessary to point out that Eq. (14) is commonly used with quasi-static material data and for fatigue purposes. In the case of the spoiler heating by the beam we are not involved in a fatigue process but in a “one-time” accident scenario. It is known that when a beam hits a material the energy is deposited very quickly into it. This causes a rapid expansion of the material, and hence quasi-static material properties will not give an accurate answer. In this case, the materials under study need to be characterised dynamically in order to give more valid results. For a more precise thermo-mechanical characterisation of the spoiler material numerical simulations are usually performed using tools such as FLUKA [21] and ANSYS [22]. Simulation results are shown in the next section.

2.1.3. *Thermo-mechanical analysis of the spoiler.* In order to evaluate the robustness of the spoiler, simulations, using the codes FLUKA and ANSYS, have been made considering the geometrical parameters of the CLIC E-spoiler made of Be, and assuming the nominal parameters of the CLIC beam.

The following horizontal and vertical beam sizes at the spoiler position have been assumed^{||}: $\sigma_x = 779 \mu\text{m}$ and $\sigma_y = 21.9 \mu\text{m}$. The bunch train impact was simulated using FLUKA. Figure 7 shows the energy deposition in the spoiler as the beam traverses it. A transverse position depth of $d \simeq 7.8 \text{ mm}$ (see Fig. 4) for the beam was chosen, to maximise the total amount of material that it would face in case of a pessimistic accident scenario. This represents a deviation of about $10 \sigma_x$ from nominal orbit. Figure 8 shows the corresponding peaks of energy density along the beam track in the spoiler material. The peak of energy deposition happens in the edge of the trailing taper and is about $5.4 \text{ GeV}/\text{cm}^3$ per incident particle; using the specific heat and density values of beryllium, shown in Table 6, and the total number of particles in a CLIC bunch train, $N_b \times N_e = 1.16 \times 10^{12}$, a temperature increment of approximately 570 K is obtained.

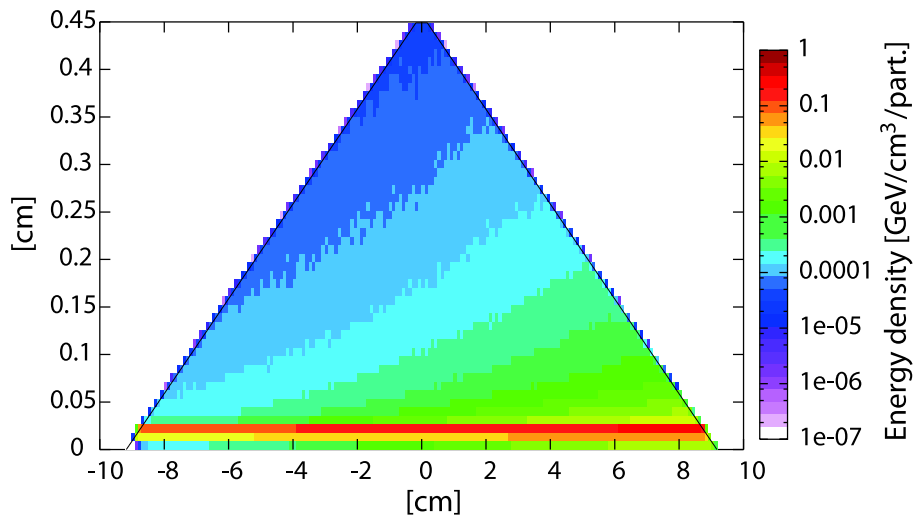


Figure 7. Energy density deposition normalised per incident particle for a CLIC beam hitting the spoiler.

In order to perform the transient analysis of the CLIC train hitting the Be E-spoiler, the FLUKA result was transformed into an ANSYS input and applied in a spoiler model. The results are recorded after the beam has hit the spoiler to determine if there would be any stress build up that could reach fracture levels. The results of the stress calculations in the Be can be compared with the mechanical stress limits of the material by means of a certain failure criterion expressed by the equivalent stress

^{||} $\sigma_x = 779 \mu\text{m}$ at spoiler position corresponds to the rms horizontal beam size of a beam with a uniform energy spread of 1% full width. However, in this FLUKA simulation we have assumed the nominal energy for all particles of the beam and no energy spread. This assumption gives more pessimistic predictions than a more realistic situation.

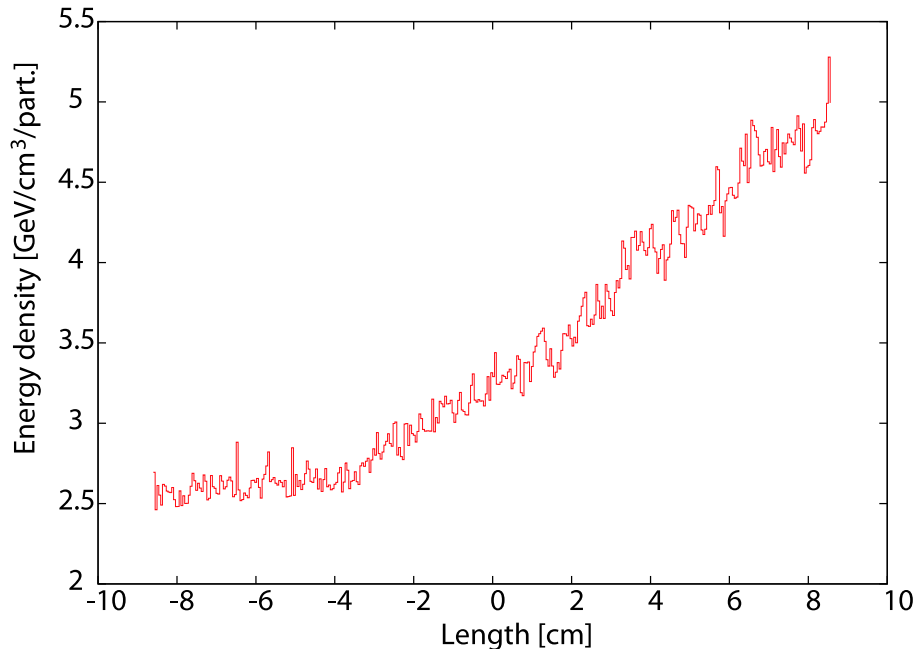


Figure 8. Peaks of energy density deposition normalised per incident particle for a CLIC beam hitting the spoiler.

values¶:

$$\sigma_{eq} = \frac{1}{\sqrt{2}} \sqrt{(\sigma_1 - \sigma_2)^2 + (\sigma_2 - \sigma_3)^2 + (\sigma_3 - \sigma_1)^2}, \quad (15)$$

where σ_1 , σ_2 and σ_3 are the principal stresses at a given position in the three main directions of the working coordinate system, which in our case is Cartesian. Figure 9 shows the equivalent stress calculated using ANSYS on the spoiler body 3 μ s after the full CLIC bunch train has hit it, time at which the stress reaches its maximum and stabilises, with an impact depth of $d \simeq 7.8$ mm. In this case we obtain a top equivalent stress of ≈ 950 MPa, and tensile, which is way above the ultimate tensile strength limit, thus reaching fracture levels.

Let us now consider another case of impact in which the beam traverses less quantity of material. For instance, the case of the beam hitting the spoiler with impact depth $d = 3.7$ mm, which means a deviation of about $5 \sigma_x$ with respect to the nominal beam axis. Figure 10 shows the equivalent stress calculated using ANSYS, after 11 μ s, the time needed in this case for the stress to reach its peak and stabilise over that top value. The maximum value of stress after a CLIC bunch train has hit the spoiler is about 240 MPa, and compressive, value that corresponds to the yield compressive strength value. In this situation there will not be fracture, but there might be a permanent deformation. This

¶ This equivalent stress is also called *von Mises stress* [23], and is often used for metals under multi-axial state stress. It allows any arbitrary three-dimensional stress state to be represented as a single positive stress value. Equivalent stress is part of the maximum equivalent stress failure theory used to predict the onset of yielding and to describe the post-yielding response.

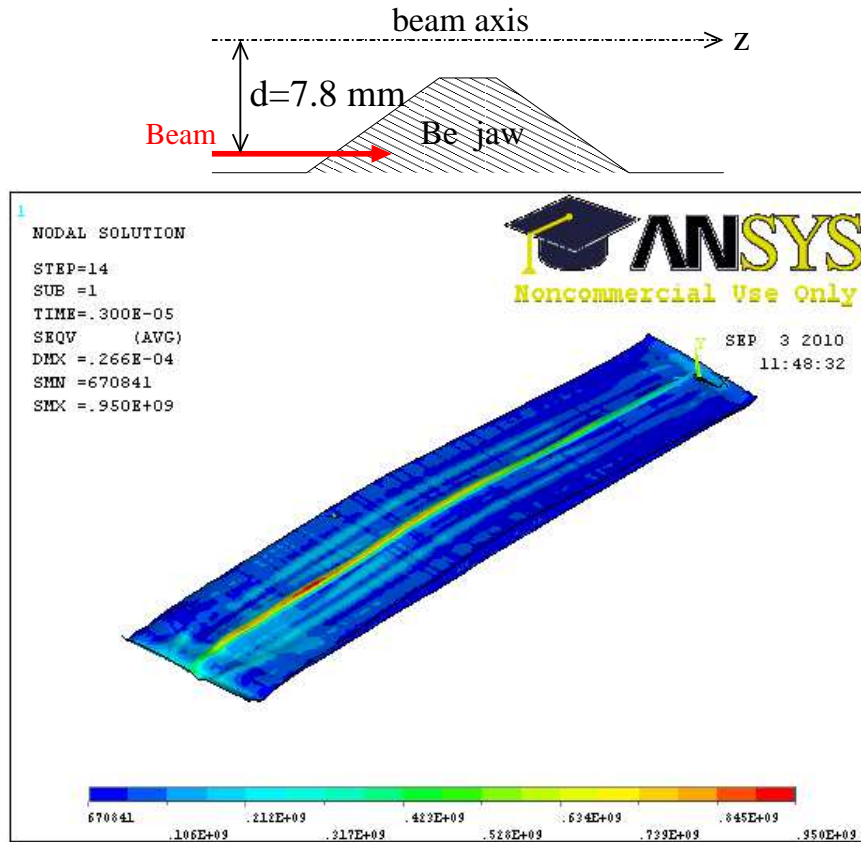


Figure 9. Equivalent stress on the spoiler body 3 microseconds after a CLIC bunch train hits it. In this case the transverse impact depth is $d = 7.8$ mm, which corresponds to a beam deviation of $10 \sigma_x$ with respect to the beam axis.

deformation translates into horizontal protuberances of $\sim 1 \mu\text{m}$, which represents 0.03% of the minimum half gap of the E-spoiler. This might have consequences in terms of degradation of the beam stability and emittance blow-up by increasing the collimator wakefield effects. The additional wakefield effects due to the deformation of the spoiler are evaluated in Section 3.3 (Part II).

Above we have considered two cases of impact position on the spoiler surface: a big transverse impact depth of about $10 \sigma_x$ from the nominal beam axis, and a more optimistic scenario with an impact depth of about $5 \sigma_x$. These two examples, one more pessimistic than the other, have allowed us to obtain a preliminary estimate of the survivability of the CLIC E-spoiler. However, the impact position of the beam on the spoiler surface depends on failure scenarios, and a detailed study of these failure events affecting the beam energy would be useful in order to determine the most likely angles and positions of impact for a more precise risk analysis.

Another necessary remark is that this study has been performed for a perfect beryllium structure, i.e. without any imperfections or impurities, which could act as a stress concentrator. Therefore, Be samples will need to be tested to compressive stress

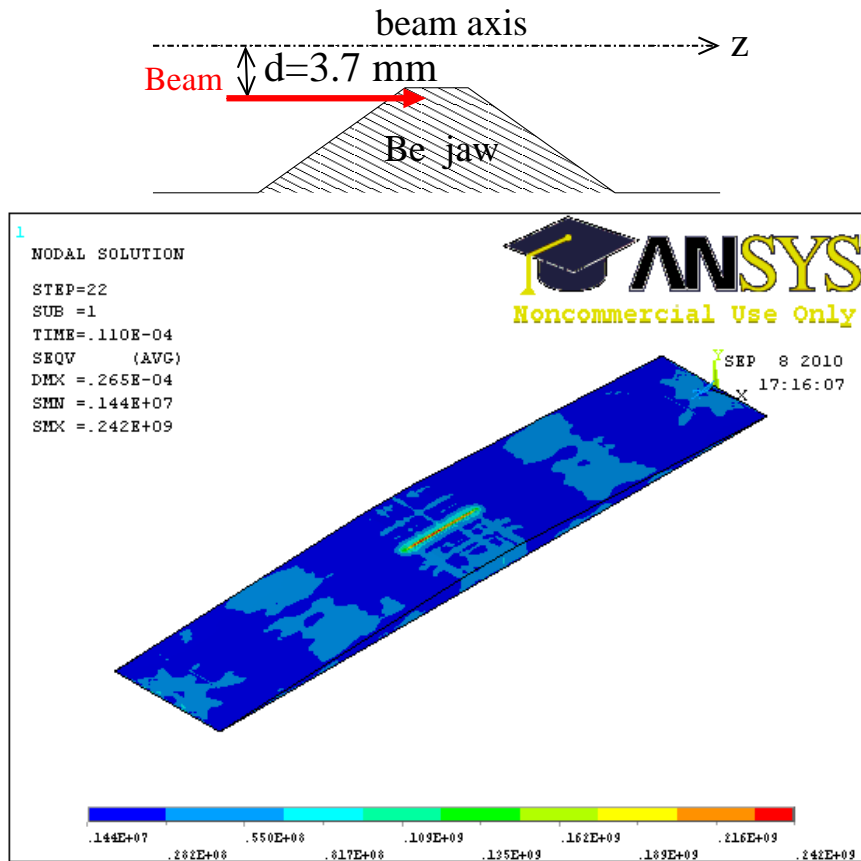


Figure 10. Equivalent stress on the spoiler body 11 microseconds after a CLIC bunch train hits it. In this case, the transverse impact depth is $d = 3.7$ mm, which corresponds to a beam deviation of $4.8 \sigma_x$ with respect to the beam axis.

up to 200 MPa to assess their suitability for spoiler manufacturing.

2.2. Collimation efficiency

In this section the capability of the system to intercept off-energy beams is investigated by means of particle tracking simulations.

Let us assume complete transmission of the beam through the E-spoiler⁺ and perfect collimation at the absorber, i.e. particles hitting the absorber are considered totally lost without production of secondary particles. With these assumptions, a beam of initial energy offset 1.5% of the nominal energy and 1% full energy spread has been tracked through the CLIC BDS using the code PLACET. Figure 11 shows the horizontal and vertical phase space at the exit of the E-spoiler, taking into account the effect of MCS for different cases of traversed spoiler length in units of radiation length (X_0). The tracking results show how the transverse beam phase space area increases at the spoiler

⁺ This approximation is only valid for very thin spoilers (less than 1 radiation length) made of materials with low Z .

exit as the spoiler length increases. In Fig. 11 (Left) the results also show that part of the beam (with x amplitude < 3.5 mm) does not hit the spoiler and is not scattered by MCS. To avoid this, if we demand a complete interception of the off-energy beam (with the above energy conditions), the E-spoiler half gap has to be reduced further, to about 2.5 mm. Reducing the spoiler half gap, the wakefield effects increase. This may be a possible cause for concern. However, as we will see in Section 3 (Part II), the contribution of the E-spoiler to the wakefields is practically negligible due to its relative large half gap (3.5 mm) in comparison with that of the betatron spoilers ($\sim 100 \mu\text{m}$), which significantly contribute to the collimator wakefields for small position offsets from the orbit axis. Reducing the E-spoiler half gap to 2.5 mm might still give a tolerable stability margin in terms of wakefields.

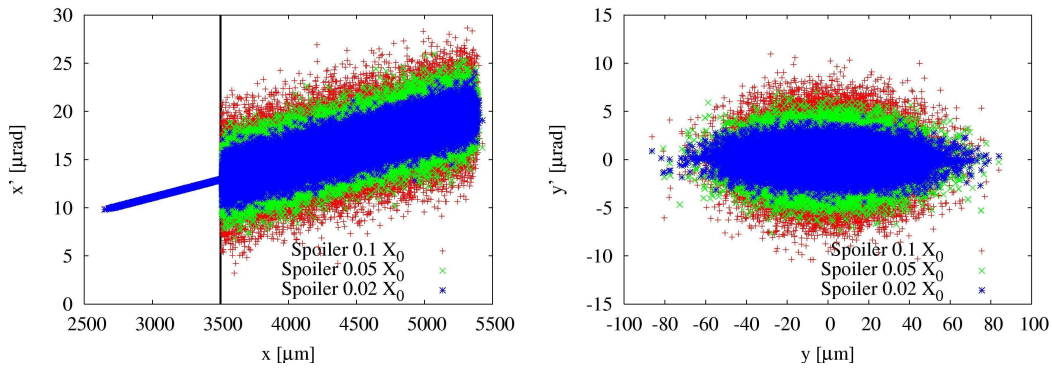


Figure 11. Left: $x-x'$ phase space at the exit of the spoiler. Right: $y-y'$ phase space at the exit of the spoiler. The following cases of traversed spoiler length are represented: $0.02 X_0$, $0.05 X_0$ and $0.1 X_0$. The collimation limit, determined by the edge of the spoiler jaw, is represented by the vertical black line.

Figure 12 shows the horizontal and vertical distribution of the beam particles at the E-absorber. Particles with amplitude $x > 5.41$ mm are perfectly absorbed. However, part of the beam does not hit the absorber jaw and is propagated downstream, with risk of hitting some sensible components of the lattice or at the interaction region. Where are these particles deposited? In order to study the efficiency of the energy collimation system to intercept a miss-steered beam with centroid energy offset $\gtrsim 1.5\%$, the particle loss map along the CLIC BDS has been studied via tracking simulations. As expected, the main particle losses are concentrated at the absorber (see Fig. 13). However, with the current absorber aperture, $a_x = 5.41$ mm, only 70% of the miss-steered beam is collimated. Considering a beam pipe radius of 8 mm in the BDS, approximately 10% of beam losses occur in a region just upstream of the E-absorber. These residual losses of primary beam particles in non-dedicated collimation places (uncontrolled losses) hit the beam-pipe or other parts of lattice elements, thus creating additional fluxes of muons and other secondary particles which propagate downstream. To avoid uncontrolled particle losses, a possible solution could be the increase of the beam pipe radius from the current

design 8 mm to a new value of about 10 mm ^{*}.

If the absorber aperture is reduced to $a_x = 4.0$ mm, practically 100% of the beam is stopped at the E-absorber.

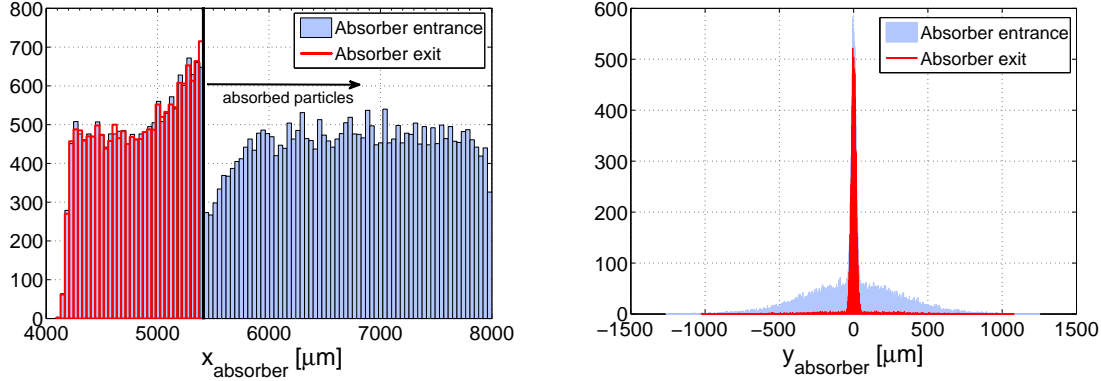


Figure 12. Transverse beam distribution at the E-absorber entrance and exit, considering a beam with 1.5% centroid energy offset and a uniform energy distribution with 1% full width of energy spread. Projection on the horizontal plane (Left), and projection on the vertical plane (Right). The collimation limit determined by the edge of the absorber jaw is represented by the vertical black line.

3. Beam diagnostics in the collimation section

It is planned to set up beam position monitors (BPMs) at every quadrupole of the CLIC BDS and, therefore, each quadrupole of the collimation system will be equipped with one BPM of about 20–50 nm resolution. Sub-micron resolution levels can be achieved by using cavity BPMs. C-band and S-band type BPMs have been successfully commissioned and tested at the KEK final focus Accelerator Test Facility (ATF2) [25], achieving resolutions in the range 20-200 nm [26]. These BPMs will play a key role in the beam based alignment procedure of the collimation system and, in general, of the whole BDS. They will further form part of the necessary equipment for the implementation of orbit feedback systems for the BDS.

Beam loss monitors (BLMs) distributed along the collimation system would be useful to quantify the beam losses. These BLMs would be integrated into a global machine protection system, which would abort machine operation or activate the necessary protection mechanisms if intolerable levels of radiation are detected. The details of this system will be specified during the technical design phase.

Another important diagnostic instrument foreseen to be located into the collimation section is the post-linac energy spectrometer. The post-linac energy measurement has been devised in a way to minimise the required space due to the tight constraints in

^{*} Parallel and complementary studies, based on resistive wall effect in the CLIC BDS, have also suggested an optimum beam pipe radius of 10 mm [24].

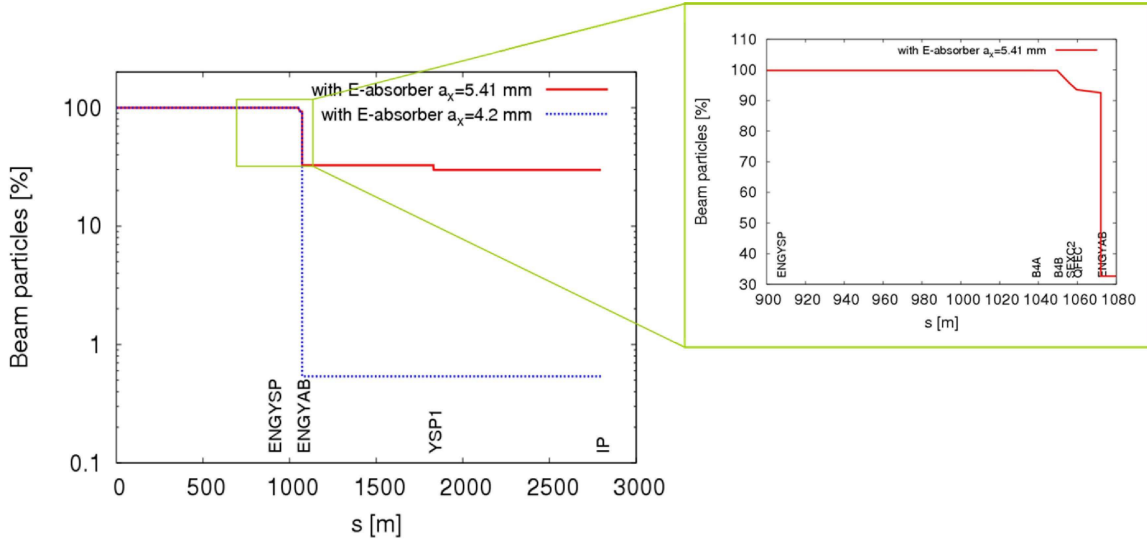


Figure 13. Left: number of beam particles along the CLIC BDS, considering an initial beam composed by 50000 macroparticles with 1.5% centroid energy offset and 1% full width of energy spread. Multiple Coulomb scattering within the E-spoiler (ENGYS) increases the angular divergence. Perfect absorption of the beam is considered at the downstream E-absorber (ENGYAB) and at other limiting apertures of the lattice. Notice the logarithmic vertical scale. The cases for E-absorber apertures $a_x = 5.41$ mm and $a_x = 4.2$ mm are shown. Right: zoom of the particle losses in the section between ENGYS and ENGYAB.

the CLIC total length. The deflection by the first dipole in the energy collimation section, together with three high precision BPMs, provides a compact spectrometer for energy measurement. A conceptual layout of this system is shown in Fig. 14. The energy measurement resolution of the set up is estimated to be $\approx 0.04\%$. The integrated magnetic field is assumed to have a calibration error of $\Delta(BL)/BL \approx 0.01\%$ and the BPM resolution is 100 nm. In addition, the energy collimation lattice incorporates a pulsed kicker magnet and a beam dump point, which can extract the beam downstream of the energy diagnostic station. This permits the linac commissioning without requiring the beam to pass through the IP.

The CLIC energy collimation section has also a suitable drift space between the collimation dipoles to locate an upstream Compton based polarimeter [27]. It consists of a laser crossing point at position $s = 742$ m and a Compton electron detector at $s = 907$ m, behind 12 dipoles. This system would allow polarimetry from 1.5 TeV down to 135 GeV beam energies, but would require several wide-aperture dipoles. If we decide to locate the detector behind a lesser number of dipoles, the dipole aperture requirement would be reduced at the expense of reducing the reachable energy range, e.g. from 1.5 TeV down to 511 GeV, if the detector is placed behind 6 dipoles from the laser position. Ref. [27] concludes that for CLIC a standard Q-switched YAG laser operated with 100 mJ/pulse at 50 Hz would give adequate polarimeter performance.

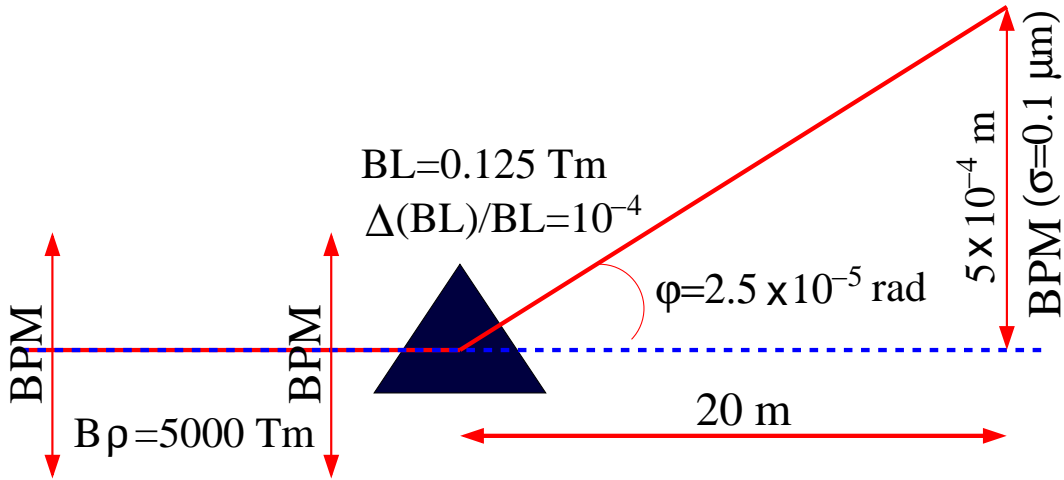


Figure 14. Conceptual compact CLIC energy measurement.

4. Summary and conclusions

The post-linac collimation system of CLIC must fulfil two main functions: the minimisation of the detector background at the IP by the removal of the beam halo, and the protection of the BDS and the interaction region against miss-steered or errant beams.

Recently several aspects of the CLIC post-linac collimation system at 3 TeV CM energy have been optimised in order to improve its performance. This report has been devoted to explain the optimisation procedure and to describe the current status of the CLIC collimation system.

The CLIC collimation system consists of two sections: one for momentum collimation and another one for betatron collimation. Next, the conclusions for the energy or momentum collimation system are summarised:

- The energy collimation system of CLIC is designed to remove particles with off-energy $\gtrsim 1.3\%$ of the nominal beam energy. Furthermore, it is conceived as a system for passive protection against beams with large energy offsets ($\gtrsim 1.3\%$), caused by likely failure modes in the main linac.
- The design and optimisation of the energy collimators (spoiler and absorber) have been based on survival conditions. The energy collimators are required to survive the impact of an entire bunch train.
- A minimum spoiler length of $0.05 X_0$ seems to provide enough transverse angular divergence by MCS to reduce the transverse beam density and guarantee the survivability of the downstream absorber in case of the impact of a bunch train.
- Beryllium has been selected to made the energy spoiler due to its high thermo-mechanical robustness as well as its high electrical conductivity (to reduce resistive wakefields) in comparison with other materials.

- Thermo-mechanical studies of the energy spoiler, based on the codes FLUKA [21] and ANSYS [22], have shown that fracture levels are reached if a bunch train hits the spoiler at $\sim 10 \sigma_x$ horizontal offset from the beam axis. In the case of a more optimistic risk scenario, when a bunch train hits the spoiler at $\sim 5 \sigma_x$, practically at the edge of the spoiler, the material does not fracture, but there might be permanent deformations. These deformations consist of horizontal protuberances of $\sim 1 \mu\text{m}$. In principle, in terms of near-axis wakefields, a rough evaluation of the consequences of these deformations indicate negligible effects. However, for a more precise evaluation, further studies of near-axis and near-wall wakefield effects are needed.
- From collimation efficiency studies, based on tracking simulations, the following conclusions can be drawn: increasing the beam pipe aperture from 8 mm to 10 mm seems to help to eliminate undesired residual beam losses in non-dedicated collimation places; reducing the energy collimator half gaps to 2.5 mm (spoiler) and 4 mm (absorber) has proved an optimal removal of beams with 1.5% mean energy offset and 1% full energy spread (for a uniform energy distribution).

Acknowledgements

This work is supported by the European Commission under the FP7 Research Infrastructures project EuCARD, grant agreement no. 227579.

References

- [1] R. Tomás, “Overview of the Compact Linear Collider”, Phys. Rev. ST-AB **13**, 014801 (2010).
- [2] F. Tecker *et al.*, “CLIC 2008 parameters”, CLIC-NOTE-764 (2008).
- [3] D. Schulte and F. Zimmermann, “Failure Modes in CLIC”, Proceedings of PAC 2001, Chicago; CLIC-NOTE-492 (2001), CERN-SL-2001-034 (AP) (2001).
- [4] NLC Design Group, “Zeroth-Order Design Report for the Next Linear Collider,” 573-574 (1996).
- [5] R. Assmann *et al.*, “Overview of the CLIC Collimation Design”, Proceedings of PAC 2001, Chicago, USA.
- [6] R. Assmann *et al.*, “Collimation for CLIC”, AIP Conf. Proc. Vo. 693, pp. 205-208, December 16, 2003.
- [7] ILC Collaboration, “International Linear Collider Reference Design Report. Volume 3: Accelerator”, ILC-REPORT-2007-001, August, 2007.
- [8] I. Agapov *et al.*, “Tracking studies of the Compact Linear Collider Collimation system”, Phys. Rev. ST-AB **12**, 081001 (2009).
- [9] L. Deacon *et al.*, “Muon backgrounds in CLIC”, Proceedings of IPAC 2010, Kyoto, Japan, 2010.
- [10] M. Jonker *et al.*, “The CLIC machine protection”, Proceedings of IPAC 2010, WEPEB71, Kyoto, Japan, 2010.
- [11] S. Fartoukh, J. B. Jeanneret and J. Pancin, “Heat deposition by transient beam passage in spoilers”, CERN-SL-2001-012 AP, CLIC Note 477, 2001.
- [12] M. Sands, “Emittance Growth from Radiation Fluctuations”, SLAC/AP-47, December 1985.
- [13] R. H. Helm, M. J. Lee and P. L. Morton, “Evaluation of Synchrotron Radiation Integrals”, SLAC-PUB-1193, March 1973.

- [14] B. Dalena *et al.*, “Solenoid and Synchrotron Radiation effects in CLIC”, Proceedings of PAC 2009, Vancouver, Canada, 2009; EuCARD-CON-2009-059.
- [15] Particle Data Group, Physics Letters B **667** (2008), p. 271.
- [16] P. Tenenbaum, “Studies of beam optics and scattering in the next linear collider post-linac collimation system”, Proceedings of LINAC 2000, MOA08, (2000).
- [17] <https://savannah.cern.ch/projects/placet>.
- [18] N. Phinney, “SLC final performance and lessons”, Proceedings of LINAC 2000, Ed. A. W. Chao, eConf C00082 (2000), MO102; arXiv:physics/0010008.
- [19] S. M. Seltzer and M. J. Berger, “Improved Procedure for Calculating the Collision Stopping Power of Elements and Compounds for Electrons and Positrons”, Int. J. Appl. Radiat. Isot. Vol **35**, No. 7, pp. 665-676 (1984).
- [20] <http://www.matweb.com>. This website, widely used by the material engineering community, provides a very reputable source of material properties.
- [21] A. Fasso *et al.*, “FLUKA: a multi-particle transport code”, CERN-2005-10 (2005), INFN/TC-05/11, SLAC-R-773.
- [22] <http://www.ansys.com/> (ANSYS® v. 11.0 Academic Research)
- [23] R. von Mises, “Mechanik der Festen Körper in plastisch deformablen Zustand,” Göttin. Nachr. Math. Phys. vol. 1, pp. 582-592 (1913). (In German).
- [24] R. Mützner *et al.*, “Multi-bunch effect of resistive wall in the CLIC BDS”, Proceedings of IPAC 2010, Kyoto, Japan, 2010.
- [25] P. Bambade *et al.*, “Present status and first results of the final focus beam line at the KEK Accelerator Test Facility”, Phys. Rev. ST-AB **13**, 042801 (2010).
- [26] S. Boogert *et al.*, “Cavity Beam Position Monitor System for ATF2”, Proceedings of IPAC 2010, Kyoto, Japan, 2010.
- [27] K. P. Schüller, “Upstream polarimeter for CLIC”, talk presented at the CLIC 2008 Workshop, CERN, Geneva, 14-17 October 2008.